M&C 2001 Salt Lake City, Utah, USA, September 2001.

DEVELOPMENT AND VALIDATION OF A METHODOLOGY FOR NEUTRON DYNAMICS ANALYSIS OF RBMK REACTORS

Jasiulevicius, A., Kubarev, A., Sehgal, B. R.
Stockholm Royal Institute of Technology (RIT)
Nuclear Power Safety Division
Dröttning Kristinas väg 33A, 100 44 Stockholm, Sweden
audrius@egi.kth.se

Keywords: RBMK, neutron dynamics, codes

ABSTRACT

This paper describes the development and validation of a methodology for neutron dynamics calculations of RBMK reactors. The aim of the work is to develop an independent reactor neutron kinetics analysis methodology. Neutron cross sections for the 3D reactor neutron dynamics calculations were obtained by employing the HELIOS code developed at Studsvik Scandpower Company. The code is widely used in the neutron cross-section generation for LWR reactors around the world. The neutron cross sections calculated with the HELIOS code were employed in the CORETRAN code to analyze a set of critical assembly experiments, performed several years ago in Russia. In addition two group cross sections were also generated for the Ignalina Nuclear Power Plant (INPP) reactor core analysis with the CORETRAN code. Thus the methodology was validated against data from the critical assemblies and the INPP.

1. INTRODUCTION

The RBMK reactors are channel type, water-cooled and graphite moderated reactors. Originally developed for plutonium production in the former Soviet Union, the first RBMK type electricity production reactor was put on-line in 1973. Currently there are 13 operating reactors of this type. Two of the RBMK-1500 reactors comprise the Ignalina NPP located in Lithuania.

1.1 Methodologies for the RBMK reactor neutron dynamics calculations

The RBMK reactor physics calculations, performed in Russia are similar to those performed for light water reactors (LWR's) in the West. The two group neutron cross section libraries are generated with the WIMS code, where the various cross sections are represented as a function of fuel and graphite temperatures, fuel burn up, Xenon-135 concentration and coolant density. A model of homogenized cell of 25x25 cm is used, having reflecting boundary conditions for a many group one - dimensional or two - dimensional neutron transport equation solution. The spectrum obtained is then employed to collapse the many group cross-sections to 2 group cross sections.

For reactor core calculations there are two codes available. The Kurchatov Institute (KI) uses the STEPAN code. The STEPAN code solves two-energy group diffusion equation in two or three - dimensional geometry. The equations are solved by either the finite-difference scheme or by using nodal approximation. The STEPAN code is coupled with KOBRA thermal hydraulic code to obtain the transient thermal hydraulic feedback or with KONTUR code for the steady state thermal hydraulic feedback. The Russian Research and Development Institute of Power Engineering (RDIPE) has developed the SADCO code, which is similar to the STEPAN code, and it also employs the 2 group cross section libraries generated with the WIMS code.

The combinations of both the STEPAN - WIMS and the SADCO - WIMS codes in general are not able to predict accurately the measured radial power distribution in the INPP. Modifications are made in the cross sections to obtain better fits to the measured power distributions. The STEPAN code changes the thermal cross sections for some assemblies while the SADCO code changes the assembly burnups, which change the cross sections for both groups and axial positions of control rods. The correction procedures employed by these two codes, are not documented and lack transparency.

An independent methodology is recently being developed at Royal Institute of Technology (RIT), Division of Nuclear Power Safety. The methodology employs Western computer codes for the RBMK reactor calculations. The two group neutron cross sections are calculated using the HELIOS code, where exact geometry of the various assemblies is employed. The core neutron dynamics calculations are performed using CORETRAN code, which uses neutron cross sections generated with HELIOS code. No corrections are made to the two group cross sections generated with the HELIOS code. The aim of this paper is to present the methodology and to describe the validation results.

1.2 RBMK-1500 reactor core description

The core of RBMK-1500 reactor is a large graphite stack (11.8 m in diameter and 7 m high). The stack is penetrated by 2052 channels. Most of these channels (the total number is 1661) contain fuel assemblies. The fuel assembly consists of two parts: upper and lower, which are placed one above another in the reactor fuel channel. There are 18 fuel pins in each fuel assembly. Besides the fuel channels there are certain number of so-called 'special purpose channels' in the core. These channels contain control rods, various detectors, etc (Almenas, 1998). The reactor fuel is a slightly enriched uranium oxide (2.4% enrichment). The fuel enrichment was increased from initial 2% level due to the safety modifications after the Chernobyl accident.

RBMK reactor power is controlled by the Control and Protection System (CPS). The system consists of two sub-systems: the standard reactor control system and Fast Acting Scram System. The CPS is cooled by an independent water circuit. In total there are 211 channels with control rods. There are 3 types of control rods: Manual Control Rods (MCR), Shortened Control Rods (SCR) and Fast Acting Scram Rods (FASR). The MCR and FASR rods are inserted from the top of the core while the SCR rods (which are employed to control axial

power distribution along the height of the core) are inserted from the bottom. The absorber used in the control rods is B_4C and Dy_2TiO_5.

2. RIT METHODOLOGY FOR RBMK REACTOR NEUTRON DYNAMICS CALCULATIONS

The neutron cross-section variation model for the RBMK applications is based on the logic shown in Fig. 1. The CORETRAN code reads a file XST.dat with HELIOS code calculated 2 group neutron cross-section data recorded in the forms of tables and performs computation of 2D polynomial coefficients. The coefficients are allocated in the dynamic computer memory during the time of CORETRAN calculations and are directly accessed each time when recalculation of each cross section is performed during the transient computations.

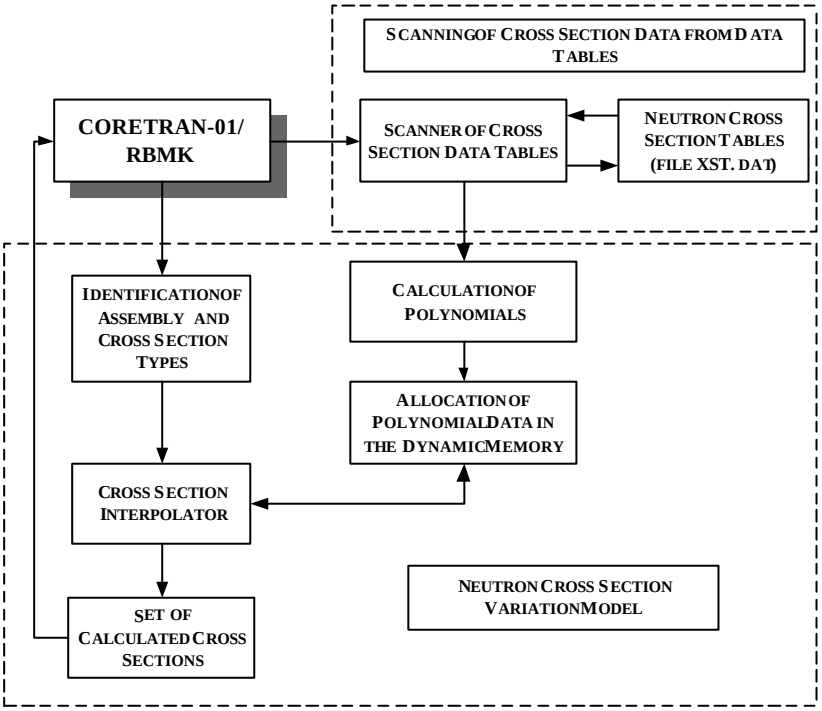

Fig. 1 Cross-section variation model

The polynomial coefficients define 2D functions for each cross - section (XS) of each assembly type. These 2D functions are used to calculate basic components in the XS variation model. The basic components are calculated by running special interpolation procedure, which performs interpolation by using polynomial coefficients. The thermal-hydraulic parameters computed in a respective calculation node by CORETRAN are considered as the reference points for the calculation of the time dependent cross sections. The basic components are summed and final change in cross sections is obtained.

The XS variation model for fuel assemblies is based on Eq. (1):

$$\Sigma (B,D_C,T_F,T_G,) = \Sigma_F(B,D_C,) + \Delta\Sigma(B,T_F,) + \Delta\Sigma(B,T_G,) \quad (1)$$

Here, $\Sigma(B,D_C,T_F,T_G,)$, the neutron cross section is a function of fuel burn up B, coolant density D_C, fuel temperature T_F and graphite temperature T_G. The value of the cross section $\Sigma(B,D_C,)$ or first basic component, is calculated by the interpolating polynomials that define XS dependence on fuel burn up B and on coolant density D_C (a 2D table where variables are B and D_C). The other two terms in Eq. (1) represent differential values coded into the 2D polynomial tables to account for the correction of cross sections due to variations of fuel and graphite temperatures versus fuel burn up. As one may notice in Eq.(1), the three terms (basic components) are assumed to be independent.

Cross sections for non-fuel assemblies are calculated by employing Eq.(2) where $\Sigma_{NF}(D_{CCPS},D_{CMCC},T_G)$ is cross section of non fuel assembly as a function of coolant presence in the CPS channel D_{CCPS}, average coolant density in the surrounding fuel channels D_{CMCC}, and graphite temperature T_G of surrounding graphite blocks.

$$\Sigma_{NF}(D_{CCPS},D_{CMCC},T_G,)= \Sigma(B,D_C,)_{DCCPS} \quad (2)$$

In order to calculate XS for non-fuel assemblies two sets of XS tables in 2D format are introduced. The first set of data accounts for XS calculated by considering conditions, when CPS system cooling water is present and the second set of data is generated by assuming that the CPS channels are empty (without coolant).

For fuel cell calculations, two sets of cross sections are to be generated for each assembly type. This is due to the reason that the upper and lower assemblies in the reactor core are not identical in the RBMK-1500 reactor. There is additional steel present in the upper assemblies. The steel is in the form of additional flow intensifiers, which increase two-phase flow mixing in the upper part of the core.

Table 1 presents a complete set of cross sections or parameters, which are obtained employing HELIOS calculations for the CORETRAN code input. For fuel assemblies the total number of parameters is 29 and for non-fuel assemblies 7 parameters are required.

Table 1 List of XS used in the HXSL-1 calculations (F-fuel, NF - non-fuel assemblies).

XS	Cross section or constant	Identification	Energy group	Assembly Type
1.	Diffusion Constant; G1	D_1	1	F & NF
2.	Diffusion Constant; G2	D_2	2	F & NF
3.	Scattering Cross Section (CS);	$\Sigma_{1\to2}$	$1\Rightarrow2$	F & NF
4.	Absorption CS; G1	$\Sigma_{a,1}$	1	F & NF
5.	Absorption CS; G2 (Without Xe)	$\Sigma_{a,2}$	2	F & NF
6.	$\nu\cdot$Fission CS; G1	$\nu_1\cdot\Sigma_{f,1}$	2	F
7.	$\nu\cdot$Fission CS; G2	$\nu_2\cdot\Sigma_{f,2}$	2	F
8.	Energy per fission (Ws/fission); G1	κ_1	1	F

9.	Energy per fission (Ws/fission); G2	κ_2	2	F
10.	Effective number of neutrons per fission; G1	ν_1	1	F
11.	Effective number of neutrons per fission; G2	ν_2	2	F
12.	Inverse neutron velocity; G1	$1/V_1$	1	F & NF
13.	Inverse neutron velocity; G2	$1/V_2$	1	F & NF
14.	Delayed neutron yield; DNG 1	β_{DNG1}	-	F
15.	Delayed neutron yield; DNG 2	β_{DNG2}	-	F
16.	Delayed neutron yield; DNG 3	β_{DNG3}	-	F
17.	Delayed neutron yield; DNG 4	β_{DNG4}	-	F
18.	Delayed neutron yield; DNG 5	β_{DNG5}	-	F
19.	Delayed neutron yield; DNG 6	β_{DNG6}	-	F
20.	Decay constant; DNG 1	λ_{DNG1}	-	F
21.	Decay constant; DNG 2	λ_{DNG2}	-	F
22.	Decay constant; DNG 3	λ_{DNG3}	-	F
23.	Decay constant; DNG 4	λ_{DNG4}	-	F
24.	Decay constant; DNG 5	λ_{DNG5}	-	F
25.	Decay constant; DNG 6	λ_{DNG6}	-	F
26.	Microscopic absorption CS of Xe^{135}; G2	$\sigma_{a\ Xe.2}$	2	F
27.	Microscopic absorption CS of Sm^{135}; G2	$\sigma_{a\ Sm.2}$	2	F
28.	Effective yield of Xe^{135} per fission	γ_{Xe}^{135}	-	F
29.	Effective yield of I^{135} per fission	γ_{I}^{135}	-	F

The HXSL-1 model performs modeling of XS variation during CORETRAN transient calculations by considering different conditions in the reactor core. Following assumptions were made during the implementation of the cross section variation model:

1. Historical coolant density was assumed to be $0.5 g/cm^3$;
2. The fuel assembly XS model assumes that cross section changes introduced by variation of coolant density, fuel temperature and graphite temperature are not dependent on each other;
3. Cross sections of non-fuel assemblies are calculated by fixing average burnup of surrounding fuel assemblies to 10MWd/kg.

2.1 A linking program between HELIOS and cross section library

The HELIOS code is developed for calculation of macroscopic neutron cross- sections; however, outputs produced by this code cannot be used directly in CORETRAN (or its cross section variation model HXSL-1). Therefore, a linking code named HELCON was developed at RIT to perform this task.

The HELCON is also aimed at facilitating automatic analysis of results produced by HELIOS. The code is equipped with flexible input, which allows accepting different changes in the HELIOS code output. Each block of results in the HELIOS output starts with data specification cards. The cards contain key information for HELCON functions. During an execution the HELCON compares the information provided in the input with the HELIOS output information, copies requested information, performs processing of data and finally records it into the data file.

3. HELIOS CODE

HELIOS is a neutron and gamma transport analysis code for a lattice with variation of burn up. Calculations by this code are performed in general in two-dimensional geometry. Neutron transport equation is solved employing current coupling and collision probability (CCCP) method. HELIOS input and output processors are the separate codes AURORA and ZENITH. The data flow between these codes is via a database that is accessed and maintained by the subroutine package HERMES (HELIOS manual, 1998).

At each calculation point (also called reactivity point), the essential results are particle fluxes and currents, and in case of a burn up or a time step, the new material number densities. Together with the nuclear-library data and the user's input it is all that is needed to obtain an output. Unlike the WIMS code, where the rather complicated geometry of the modeled cell is homogenized and reduced to concentric cylindrical structures, the HELIOS code allows to accurately model even very complicated structures, fully representing the cell geometry.

3.1 Models developed for RBMK-1500 reactor cell calculations

As it was already discussed, the macroscopic cross-sections for fuel and non-fuel assemblies (later referred as cells) have to be calculated by introducing different models. Therefore, two types of models were developed for HELIOS calculation.

The first model represents the fuel cell. During the calculation of cross sections the fuel cell is treated as a stand-alone cell with mirror boundary conditions. The different sets of cross sections are obtained by varying coolant density, fuel temperature and graphite temperature.

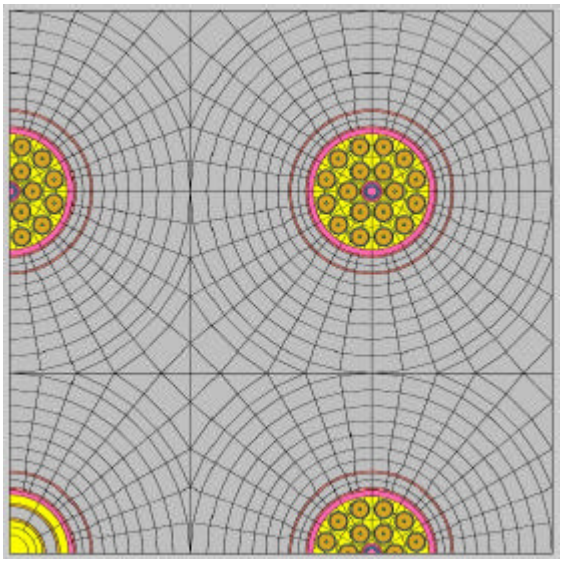

Fig. 2 Illustration of Quarter 3X3 Macro-Cell nodalization model used in actual HELIOS calculations for non-fuel cells

A second model is developed to facilitate calculation of the cross sections for the non-fuel assemblies. The non-fuel cells do not contain source of neutrons; therefore, these cells have to be surrounded by 8 fuel cells (sources of neutrons). Example HELIOS nodalization is presented in Fig. 2 for a non-fuel cell.

The macroscopic cross sections for non-fuel assemblies are calculated by extracting the non-fuel area and using neutron flux spectrum generated by surrounding fuel cells. Required collections of cross-sections are obtained by varying coolant density in the surrounding fuel channels, graphite temperature, and coolant density in the non-fuel channel. It should be noted that the graphite temperature is assumed to be uniform in the whole macro-cell and fuel burn up is fixed at 10MWd/kg.

3.2 HELIOS calculation results for fuel cell model

The recent reactor units in the INPP are loaded with two main fuel types: 2.00% U-235 enriched fuel and 2.40% U-235 enriched fuel with 0.41% erbium as a burnable poison. Er is introduced to reduce the positive void reactivity coefficient, which is a specific feature of the RBMK reactors. In future there are plans to introduce 2.6% U-235 enriched fuel with additional 0.5 % of Er. This would help to reach even lower positive void reactivity coefficients and will allow increased burn up of the fuel in the reactor. The HELIOS neutron cross sections were generated for all of the types of fuel assemblies, which are present in the reactor. The HELIOS calculation results, presented in this paper were compared against those calculated using WIMS-D_4 code. The calculation conditions were defined as follows: coolant density 0.5g/cm^3; fuel temperature 1000Kand graphite temperature 750K.

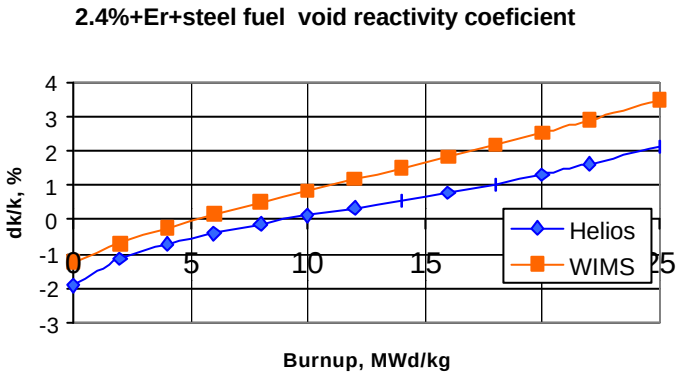

Fig. 3 Void reactivity effect in the fuel cell (2.0% U-235 enriched fuel)

Figure 3 presents an example: calculated void reactivity effect results from both codes and their comparison. The effect is calculated as:

$$dk/k=\alpha_v=(K_{inf1}-K_{inf2})/K_{inf1},\ \% \qquad (3)$$

As it is seen from the Fig.3, HELIOS predicts lower void reactivity effect as compared to that by the WIMS code. The analysis of the data showed that both codes provide very close

predictions for K_{inf} when there is a considerable amount of coolant in the fuel channels. But for a high void content in the channel, HELIOS estimates lower K_{inf} than the WIMS code.

The fuel and graphite reactivity coefficient calculations, presented in Fig.4 and Fig. 5, are calculated using the following formulas:

$$\alpha_f = (K_{inf1} - K_{inf2})/(T_{f1} - T_{f2}) \quad (5)$$

$$\alpha_g = (K_{inf1} - K_{inf2})/(T_{g1} - T_{g2}) \quad (6)$$

Here T_f and T_g are the fuel and the graphite temperatures.

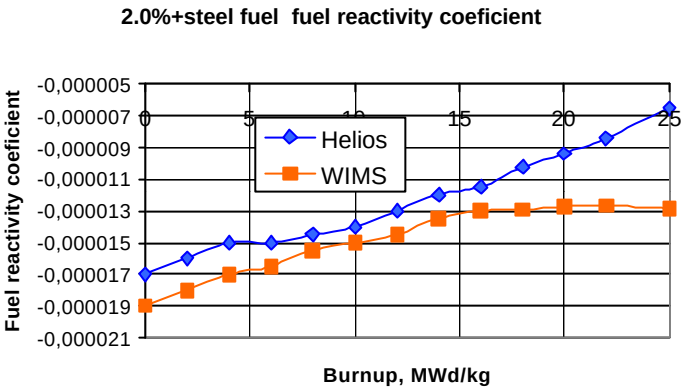

Fig. 4 Comparison of HELIOS and WIMS results for fuel reactivity coefficient calculations.

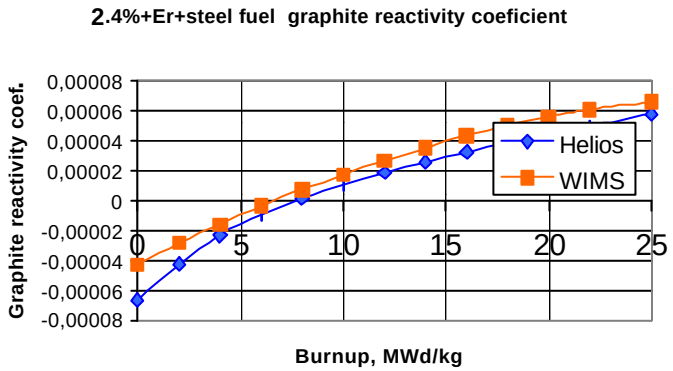

Fig. 5 Comparison of graphite reactivity coefficient

The HELIOS code yields lower K_{inf}. The differences between the two codes grow as the fuel burn up increases. But for the nominal operating burn up value (which for the RBMK reactor is around 10 MWd/kg) the agreement between the predictions of the two codes is rather good. Graphite temperature reactivity coefficient (Fig. 5) calculated using HELIOS code

agrees well with the WIMS code predictions, although the HELIOS coefficient is slightly lower than the WIMS code results.

3.3 HELIOS calculation results by employing macro-cell model

For the non-fuel cell calculations, the sets of neutron cross sections were obtained by varying the coolant density and the graphite temperature in the surrounding fuel channels, and the coolant density in the non-fuel channel. The HELIOS results for different cross sections were compared against these obtained with the WIMS-D_4 code. The example results (for the Manual Control Rod (MCR) absorber) are presented in Table 2.

Table 2 Comparison of HELIOS and WIMS calculated cross sections for MCR absorber

Const.	With coolant in CPS			Without coolant in CPS		
	WIMS	HELIOS	Discrepancy, %	WIMS	HELIOS	Discrepancy, %
D_1	1,0792	1,1053	*2,4%*	1,1229	1,1477	*2,2%*
D_2	0,8102	0,7991	*-1,4%*	0,8579	0,8499	*-0,9%*
$S_{1->2}$	5,6859E-03	5,9661E-03	*4,7%*	3,4931E-03	3,8057E-03	*8,2%*
S_{a1}	2,4187E-03	2,5686E-03	*5,8%*	2,6128E-03	2,7714E-03	*5,7%*
S_{a2}	5,6704E-03	5,7513E-03	*1,4%*	6,3767E-03	6,2588E-03	*-1,9%*

In general, as it can be seen from the example in the Table 2, the HELIOS calculated cross sections are in close agreement with WIMS code results, with the discrepancies remaining less than of 10% for all main types of non-fuel assemblies.

4. HELIOS DATABASE VALIDATION WITH THE EXPERIMENTAL CRITICAL FACILITY EXPERIMENTS

An RBMK Critical Facility is located in the Kurchatov Institute in Moscow, Russia. The design of the facility is based on the prototype of the RBMK reactor. The facility itself is a stack of a 25x25 cm graphite blocks with 11.4 cm diameter openings for channels in the center. There are 324 channels in the Facility. Different fuel channel and control rods configurations could be arranged within the graphite stack. The height of the graphite stack is 346 cm. The aim of the facility is to provide experimental data for neutron flux distributions and for core reactivity changes in the RBMK type reactors (Davidova, 1995)

4.1 CORETRAN model of Experimental Critical Facility (ECF)

Several experiments performed on the critical facility have been modeled and analyzed. Calculated results were compared to the measured data. In the CORETRAN model the critical facility core was divided into 18x18x21 rectangular nodes (21 is the number of axial nodes along the height of the assembly). As a boundary condition, no neutron flux on the boundary was chosen. During the calculation phase, radial neutron flux distribution in the assembly, axial

neutron flux distribution along the height of certain channels (corresponding to the channels in the ECF, in which the axial neutron flux distribution was recorded) was determined. The CORETRAN results were compared to the experimental data. The relative neutron flux distribution during experiments was determined using measurements of the activity of copper foils, irradiated in the core of ECF. In order to evaluate the calculated results in the same manner, relative activity of the copper foils was evaluated from the CORETRAN code by calculating relative absorption reaction rate in the copper foils (Romas, 2000):

$$A_{\alpha}=\Phi_1\sigma_{a1}+\Phi_2\sigma_{a2} \qquad (6)$$

The relative activities of the copper foils were normalized and compared to the measured values. According the experiment report (Davidova, 1995) the measurement error of the radial neutron flux distribution in the experiment was 1.5% - 2%. For some experiments, due to non-uniform distribution of U-235 isotope in the channels, the error could be as high as 7%. Besides the spatial neutron flux distribution, criticality factor keff was compared. The error of the criticality measurements during experiments was $0.0005\beta_{eff}$..

4.2 CORETRAN calculation results

The assembly included 18 fuel bundles, with 2.0% U-235 enrichment. The configuration of the assembly is shown in the Fig. 6. The fuel channels were filled with water during the experiment. Control rod and reflector (empty) channels were dry. Criticality was reached with control rods inserted to 235 cm, 240 cm (two rods) and 240 cm.

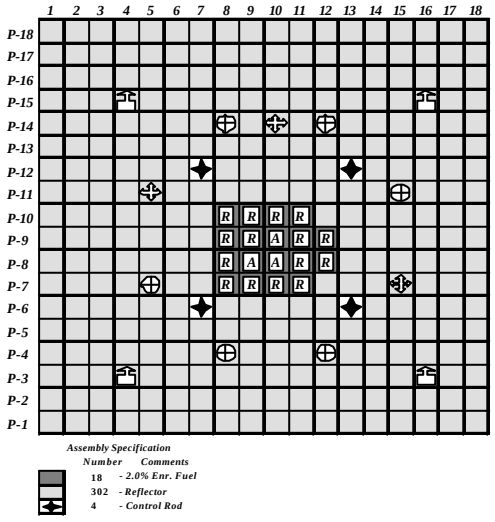

80,0	**100,0**	**104,0**	**92,0**	**Measured**
76,9	*97,8*	*103,1*	*90,9*	*Calculated*
-4,0	*-2,3*	*-0,8*	*-1,2*	***Discrepancy, %***

95,0	**123,0**	**129,0**	**112,0**	**82,0**
94,1	*120,8*	*128,0*	*112,2*	*82,5*
-0,9	*-1,8*	*-0,8*	*0,2*	*0,6*
93,0	**121,0**	**127,0**	**111,0**	**79,0**
93,0	*120,1*	*127,4*	*111,6*	*81,6*
0,0	*-0,8*	*0,3*	*0,6*	*3,2*

74,0	**90,0**	**98,0**	**90,0**
73,4	*95,8*	*101,7*	*89,2*
-0,8	*6,0*	*3,6*	*-0,9*

Fig. 6 Assembly N1 of the Experimental Critical Facility and comparison of neutron flux distribution

CORETRAN calculated effective multiplication factor was k_{eff}. = 0.9998. Radial neutron flux was measured by positioning cooper foils in all 18 fuel channels at three elevations

(90, 162 and 270 cm).The values at 3 axial measurement points were normalized by the average neutron flux. CORETRAN calculated neutron flux distribution is shown in Fig. 6. Calculated results are in good agreement with the experiment data. The axial neutron flux distribution results are presented in Fig.7. The experimental curve was obtained by averaging axial neutron distribution in three channels. CORETRAN results are an average axial neutron flux in the 3 fuel channels.

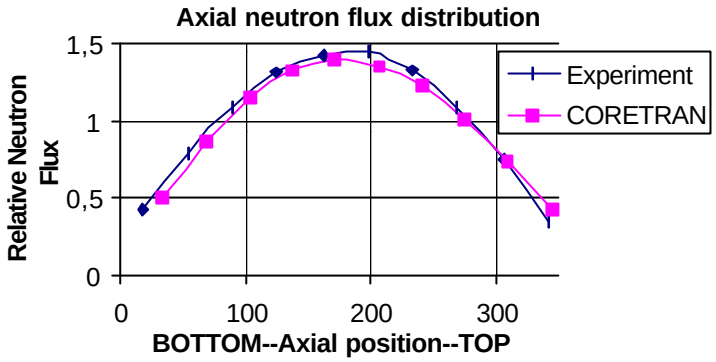

Fig. 7 Axial neutron flux distribution

Excess criticality measurements were performed using the following technique: in the initial critical state all 4 control rods were inserted 2.5 m into the core. To determine the excess criticality, some of the rods were withdrawn, keeping the same position of the remaining rods. Then the initial state and positions of all control rods is restored and the rods, which were not moved at previous measurement are withdrawn. Position of remaining rods does not change. Excess criticality for the whole assembly without control rods is determined as the sum of effects of both measurements.

For withdrawal of three control rods P6-13, P12-7 and P12-13 the measured reactivity of the system was $\rho=0.23\beta_{eff}$.. For the withdrawal of the rod P6-7 the reactivity was $\rho=0.18\beta_{eff}$.. Total sum reactivity of the system without the control rods then is equal to $\rho=0.41\beta_{eff}$.. CORETRAN calculations indicated the excess reactivity for the whole assembly equal to $\rho= 0.456\ \beta_{eff}$.. For three control rods withdrawn (P6-13, P12-7 and P12-13) calculated reactivity is $0.255\beta_{eff}$.. For the withdrawal of rod P6-7 calculated reactivity was $0.201\beta_{eff}$..

Figure 8 shows comparison of the radial neutron flux distribution for a larger critical assembly. A good agreement between calculated and measured values should be noted (it must be pointed out that the measurement error during the experiments was up to 7%).

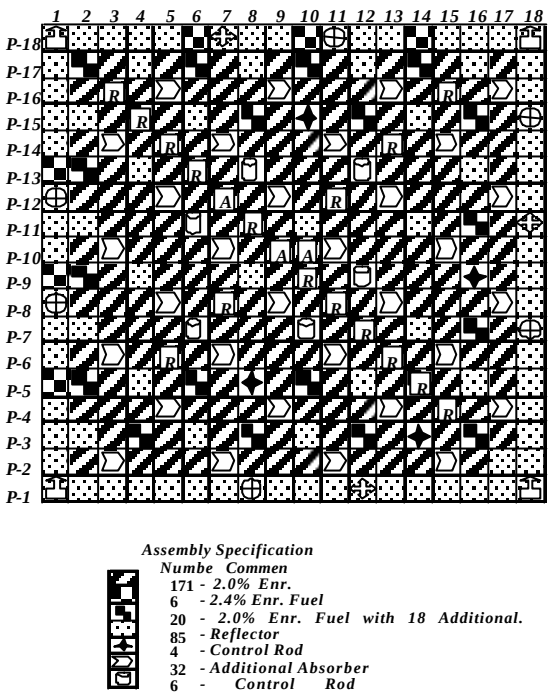

Coordinate	Exp.relative value	Calc.relative value	Deviation, %
P16-3	0.49	0.59	14.26
P15-4	0.79	0.90	12.18
P14-5	1.05	1.16	9.71
P13-6	1.04	1.05	0.96
P12-7	1.02	0.95	-7.51
P11-8	1.27	1.20	-5.46
P10-9	1.52	1.48	-2.88
P10-10	1.39	1.34	-4.01
P13-11	1.29	1.16	-11.19
P14-13	0.99	0.91	-8.95
P16-15	0.60	0.63	4.10
P6-5	0.73	0.79	8.07
P8-7	1.11	1.09	-2.19
P9-10	1.26	1.19	-5.69
P8-11	1.03	0.93	-10.95
P7-12	1.03	1.02	-0.70
P6-13	1.06	1.16	8.38
P5-14	0.80	0.87	8.04
P4-15	0.52	0.56	7.14

Fig. 8 ECF N9 assembly radial neutron flux distribution

A higher discrepancy (more than 14%) between experiment and calculated results can be noticed in the periphery of the assembly.

5. CORETRAN 3-D NEUTRON KINETICS MODEL OF RBMK-1500 REACTOR

An initial validation process of the HELIOS neutron cross-section library was performed employing CORETRAN 3-D neutron kinetics code with the new library. During the operation of the Ignalina NPP, at periodic intervals measurements of some important operational parameters, e.g. steam void coefficients are performed.

Also it is possible to obtain recorded data for the reactor state for each day, where the sensor readings allow calculating actual radial and axial power distribution in the operating reactor. This data allows testing the existing model under operating reactor conditions.

A series of such calculations were performed at RIT, comparing results obtained with the CORETRAN code against data from both reactors at the Ignalina NPP (INPP-1 and INPP-2).

Table 3 Comparison CORETRAN and STEPAN results for RBMK-1500 reactor

Unit, Data	*Code*	α_j, %	$\alpha_w \cdot 10^5$, 1/MWt	$\alpha_t \cdot 10^5$, 1/°C	$\alpha_c \cdot 10^5$, 1/°C	Δr_{MCC}, %	Δr_{CPS}, %
2-29.03.99	STEPAN	0.30	-2.30	-1.10	4.10	0.40	1.40
____ "____	CORETRAN-WIMS	0.49	-1.40	-1.75	4.12	0.75	1.34
____ "____	CORETRAN-HELIOS	0.52	-1.38	-	-	-	-
____ "____	Experiment	0.54±0.12	-1.26±0.12	-	-	-	-
2-21.12.99	STEPAN	0.20	-2.50	-1.00	4.00	0.20	1.20
____ "____	CORETRAN-WIMS	0.52	-1.32	-1.75	4.19	0.58	1.17
____ "____	CORETRAN-HELIOS	0.34	-1.51	-1.76	3.60	0.25	0.76
____ "____	Experiment	0.36±0.12	-1.56±0.12	-	-	-	

Table 3 presents the comparison of the measured data at the Ignalina NPP (for Unit 1 and Unit 2) with CORETRAN code results. The calculations using new HELIOS neutron cross section library were also compared against the same 3-D neutron kinetics calculations, but using cross section library, generated using WIMS code, which is already widely used in RBMK reactor applications, and against STEPAN code results. In most cases, the calculations, performed with new HELIOS cross-section library, give a better agreement with the experiment data. Here $a_j, a_w, a_t, a_C, \Delta r_{MCC}, \Delta r_{CPS}$ are respectively the void coefficient, the power coefficient, the Doppler coefficient, the graphite temperature coefficient, the MMC voiding effect and the CPS voiding effect.

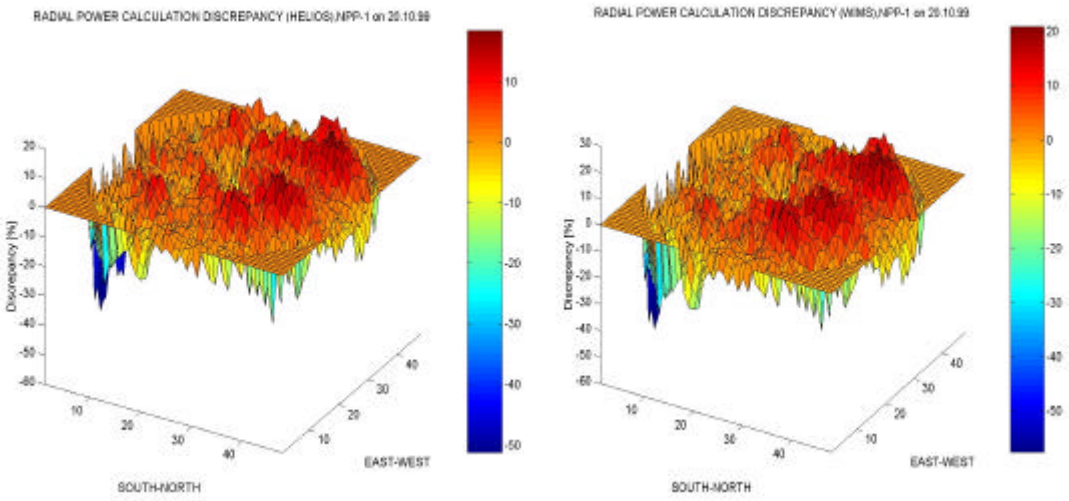

Fig. 9 Discrepancy of the radial power distribution in the INPP calculated with the CORETRAN code employing the HELIOS and WIMS neutron cross-section libraries

In Figure 9 a comparison of deviations between NPP data and CORETRAN calculations with HELIOS and WIMS cross section libraries is given. Both calculations provide quite similar radial core power distribution.

6. DISCUSSION

In this paper a methodology developed at the Royal Institute of Technology, Nuclear Power Safety Division, is presented. The methodology allows performing a completely independent RBMK reactor core 3-D neutron kinetics analysis using CORETRAN 3-D neutron kinetics code with HELIOS neutron cross-section library. The lattice calculations were performed with the HELIOS code and macroscopic neutron cross-section library was generated for all main types of RBMK fuel and special purpose channels. The results of HELIOS code calculations were compared against those with the WIMS-D_4 code. The lattice code has been used for a long time for RBMK reactor calculations.

Fuel and graphite reactivity coefficients, void reactivity effects for various type of fuel in the RBMK-1500 reactor follow the same trend as for the WIMS code results. HELIOS results for non-fuel cell calculation are also in close agreement with the values provided using WIMS code, with the deviation for the main types of the non-fuel channel macroscopic cross sections being less than 10%.

Validation, performed using CORETRAN 3-D neutron kinetics code with cross sections, generated using HELIOS code against Critical Assemblies and INPP data show very good agreement. The comparisons were performed for radial and axial neutron flux distributions as well as for core reactivity and reactivity coefficients.

NOMENCLATURE

RBMK Russian acronym for “Large Power Boiling Reactor”
CPS Control and Protection System
ECF Experimental Critical Facility
FASR Fast Acting Scram Rods
MCR Manual Control Rods
NPP Nuclear Power Plant
RIT Royal Institute of Technology
SCR Shortened Control Rods
XS cross-section
A_α relative activity of the copper foil
B burn up
D neutron diffusion cross section
K multiplication factor in the infinite state (eigenvalue)
T temperature, K
Φ neutron flux
$\nu\Sigma$ neutron generation cross-section
σ microscopic neutron cross sections

Σ macroscopic neutron cross section

Subscripts

1 1st (fast) neutron energy group
2 2nd (thermal) neutron energy group
a absorption
c coolant
f fuel
g graphite
inf infinite
s scattering (cross-section)
r removal (cross-section)

ACKNOWLEDGMENTS

The work is being carried out under the contract with the Swedish International Projects (SiP). The authors are grateful to Lic. Antanas Romas who had performed a tremendous work during the initial stages of the project.

REFERENCES

Almenas, K., Kaliatka, A., Uspuras, E., 1998. *Ignalina RBMK-1500. A Source Book*. Ignalina Safety Analysis Group, Lithuanian Energy Insitute, Kaunas.

Davidova, G. B., Kachanov, V. M., 1995. *Experiments on the RBMK Critical Facility. Data for calculation modeling*. Kurchatov Insitute, Moscow (in Russian).

Romas, A., 1999. *Development, Validation and Application of an RBMK Reactor Physics Capability at KTH*. Engineering Licentiate Thesis. Royal Institute of Technology, Stockholm.

Studsvik Scandpower. HELIOS Documentation. User's manuals. 1998